Intranight optical variability of TeV blazars with parsec-scale jets dominated by slow-moving radio knots

Vibhore Negi [ORCID],[1,2]* Gopal-Krishna,[3] Hum Chand[4] and Silke Britzen[5]

[1]*Aryabhatta Research Institute of Observational Sciences (ARIES), Manora Peak, Nainital 263002, India*
[2]*Department of Physics, Deen Dayal Upadhyaya Gorakhpur University, Gorakhpur 273009, India*
[3]*UM-DAE Centre for Excellence in Basic Sciences, Vidyanagari, Mumbai 400098, India*
[4]*Department of Physics and Astronomical Sciences, Central University of Himachal Pradesh (CUHP), Dharamshala 176215, India*
[5]*Max-Planck-Institut f. Radioastronomie, Auf den Huegel 69, D-53121 Bonn, Germany*

ABSTRACT

BL Lac objects detected at TeV energies preferentially belong to the subclass called 'high-frequency-peaked' BL Lacs (HBLs). Parsec-scale radio jets in these TeV-HBLs often show dominant, slow-moving radio knots that are at most mildly superluminal. We report the first systematic campaign to characterize the intranight optical variability (INOV) of TeV-HBLs using a representative sample of six such sources, all showing a fairly high degree of optical polarization. Our campaign consists of high-sensitivity monitoring of this sample in 24 sessions of more than 3 h duration each. For these TeV-HBLs, we find a striking lack of INOV and based on this, we discuss the importance of superluminal motion of the radio knots vis-a-vis the optical polarization, as the key diagnostic for INOV detection.

Key words: galaxies: active – BL Lacertae objects: general – galaxies: jets – galaxies: photometry – quasars: general.

1 INTRODUCTION

Quasars whose observed radiation at centimetre and shorter wavelengths arises predominantly from a jet producing non-thermal radiation relativistically beamed towards the observer are termed as blazars. They exhibit flux variability across the electromagnetic spectrum on diverse time-scales (reviewed, e.g. by Wagner & Witzel 1995; Ulrich, Maraschi & Urry 1997; Marscher 2016; Blandford, Meier & Readhead 2019). Spectroscopically, blazar population is subdivided between 'broad-line emitting' flat-spectrum radio quasars (FSRQs) and BL Lac objects (BL Lacs) showing an almost featureless optical/ultraviolet (UV) spectrum (Stickel et al. 1991), excepting the few cases for which spectral features due to host galaxy have been detected. Blazars with synchrotron emission peaking at high frequencies, between UV and X-ray bands, i.e. $\nu_{\rm syn}^{\rm peak} > 10^{15}$ Hz are most commonly BL Lacs and these are called HBLs (e.g. reviews by Antonucci 1993; Padovani & Giommi 1995; Urry & Padovani 1995; Tadhunter 2016). Compared to the BL Lacs with synchrotron spectra peaking below $\sim 10^{14}$ Hz (called LBLs, Padovani & Giommi 1995; Abdo et al. 2010), HBLs are preferentially detected at TeV energies and a few dozen such TeV-HBLs have been catalogued (Wakely & Horan 2008). HBLs typically have modest intrinsic radio luminosities, as compared to LBLs and are usually hosted by 'low-excitation radio galaxies', whose central engines are powered by radiatively inefficient gas accretion on to the central supermassive black holes (see e.g. Ghisellini & Celotti 2001; Ghisellini, Tavecchio & Chiaberge 2005; Ghisellini, Maraschi & Tavecchio 2009; Meyer et al. 2011; Giommi et al. 2012; Sbarrato, Padovani & Ghisellini 2014).

It is commonly believed that the parent (i.e. misaligned) population of BL Lacs is Fanaroff–Riley type I (FR I; Fanaroff & Riley 1974) radio galaxies (e.g. Wardle, Moore & Angel 1984; Barthel 1989; Browne 1989; Antonucci 1993; Urry & Padovani 1995). Chiaberge, Capetti & Celotti (1999) showed that relativistic beaming, rather than obscuration, of the nuclear jets can account for the $10 - 10^4$ difference in radio and optical luminosities between BL Lacs and FR I radio galaxies and the required beaming typically needs bulk Lorentz factors of just a few (e.g. Urry & Padovani 1991; Chiaberge et al. 1999; Laing et al. 1999; Hardcastle et al. 2003; Trussoni et al. 2003).

The transverse dual-velocity structure of jets was independently hypothesized by Chiaberge et al. (2000) taking into account the observed correlation between the radio and the optical core luminosity in FR I radio galaxies and BL Lacs. A more direct evidence for the 'spine-sheath' jet scenario comes from the observed limb-brightening of parsec-scale jets in several lower-luminosity radio sources, e.g. the HBLs Mrk 421 and Mrk 501 (Giroletti et al. 2004, 2006; Piner et al. 2009; Piner, Pant & Edwards 2010; Britzen et al. 2021, Bruni et al. 2021; Janssen et al. 2021; Britzen et al. 2023), and also in some kiloparsec-scale jets (Owen, Hardee & Cornwell 1989; Swain, Bridle & Baum 1998; Laing et al. 2011). Another well-documented manifestation of blazar activity is their intranight optical variability (INOV; Gopal-Krishna & Wiita 2018, and references therein; Mishra et al. 2021; Gopal-Krishna et al. 2023). At least in the context of blazars, INOV is believed to arise mainly due to a combination of two factors: (i) generation of turbulence within the jet plasma whose synchrotron emissivity and fractional polarization can increase while passing through one or more shocks (Marscher 2014 and references therein; Calafut & Wiita 2015; also Laing 1980; Goyal et al. 2012) and (ii) Doppler factor $\delta_{\rm j}$ of the post-shock turbulent jet

* E-mail: vibhore@aries.res.in, vibhore.negi18@gmail.com

plasma. While the former condition is crucial for inducing micro-variability, the latter can play a key role in making it detectable (via a Doppler boost). A strong dependence of INOV on fractional optical polarization (p_{opt}) was first established by Goyal et al. (2012), who showed that a flat/inverted radio spectrum by itself does not ensure a strong tendency for INOV. The question remains whether p_{opt} alone suffices, or the other factor mentioned above, namely, a strong beaming as inferred from the apparent speed of the VLBI radio knots, also plays a dominant role? Since, to our knowledge, no systematic investigation of this issue has been reported, we have carried out an INOV campaign targeting representative sample of six TeV blazars. The crucial aspect of these blazars is that even though they fall within the high polarization class (HPQ), their nuclear jets are dominated by radio knots showing at most mildly superluminal motion which is statistically consistent with zero radial velocity from the core, in a majority of cases (see Table 1). The selection of the sample representing this extreme subset of HPQs is described in Section 2. The observations and data reduction procedures are outlined in Sections 3 and 4. Section 5 presents the results together with a brief discussion. Our main conclusions are summarized in Section 6.

2 SAMPLE SELECTION

For the purpose of (optical) differential aperture-photometry, the present sample of six TeV-HBLs (Table 1) has been drawn from the VLBI data published in Piner & Edwards (2018) for a sample of 38 TeV-HBLs. We imposed a limit of $z \gtrsim 0.3$, in order to minimize the relative contribution from the host galaxy and thereby the possibility of claiming spurious INOV detection, in case the 'point spread function' (PSF) changes during the monitoring session (Cellone, Romero & Combi 2000). This resulted in exclusion of 30 of the sources. Another two sources got discarded due to the second filter, imposed by observational considerations, namely (i) declination > 0 and (ii) $m_r \leq 17.50$-mag, taking m_r from the Pan-STARRS DR1 (Chambers et al. 2016). This left us with a sample of six VLBI monitored TeV-HBLs (Table 1). It is seen that for only two of the six sources, J0507+6737 and J1427+2348, the estimated β_{app} deviates from zero by more than $\sim 2\sigma$, the most deviant being J0507+6737 for which the deviation is significant at 5.1σ (but, even in this case, the motion is only mildly superluminal).

3 THE MONITORING AND DATA REDUCTION

The sample of six TeV-HBLs was monitored in Johnson–Cousins R band in 24 sessions (i.e. four sessions per source), using the 1.3-metre Devasthal Fast Optical Telescope (DFOT; Sagar et al. 2011) located at Devasthal station of ARIES (India). The images were recorded on a Peltier-cooled ANDOR CCD having 2k × 2k (0.53 arcsec pixel^{-1}) pixels, covering a field of view of 18.5 × 18.5 arcmin^2. The CCD detector has a gain of 2 e$^-$ per analogue-to-digital unit and a readout noise of 7 e$^-$ at a speed of 1000 kHz. In each session, one target blazar was monitored continuously for minimum 3 h, with a typical exposure of 1.5–5 min per frame.

The pre-processing and cleaning of the CCD frames was done following the standard procedures in IRAF. The instrumental magnitude of the blazar and the two (steady appearing) comparison stars contained in all the CCD frames taken in the session were determined by aperture photometry (see Stetson 1987, 1992), using the DAOPHOT II (Dominion Astronomical Observatory Photometry II) package. The PSF was estimated by averaging the full width at half-maximum of the Gaussians fitted to the brightness profiles of five moderately

bright stars within each frame, and aperture radius was set equal to two times the PSF (see e.g. Ojha, Krishna & Chand 2019). The variation of PSF during each session is plotted in the bottom panel in the online Figs S1–S6. For each session, we then derived differential light curves (DLCs) for all pairs involving the target blazar and the chosen two comparison stars (Figs S1–S6 and Tables S1 and S2 available online as Supporting Information).

4 STATISTICAL ANALYSIS

To ascertain the presence of INOV in our TeV-HBL sample, we applied the widely used F_η test (de Diego 2010), following the basic procedure described in Mishra et al. (2019) and Chand et al. (2022). The two steady comparison stars were chosen by inspecting several star–star DLCs derived for each session and the F_η test was applied to the DLCs of the target blazar relative to the two comparison stars (whose basic parameters are listed in the online Table S2). The F-values for the two blazar DLCs of a session are computed as

$$F_1^\eta = \frac{\text{Var}(q - s1)}{\eta^2 \sum_{i=1}^N \sigma_{i,\text{err}}^2 (q - s1)/N}, F_2^\eta = \frac{\text{Var}(q - s2)}{\eta^2 \sum_{i=1}^N \sigma_{i,\text{err}}^2 (q - s2)/N} \tag{1}$$

where $\text{Var}(q - s1)$ and $\text{Var}(q - s2)$ are the variances of the two DLCs of the target blazar, and $\sigma_{i,\text{err}}(q - s1)$ & $\sigma_{i,\text{err}}(q - s2)$ represent the rms error returned by DAOPHOT on the ith data point in a DLC of the target blazar. N is number of data points in the DLCs and the scaling factor $\eta = 1.54$ (Gopal-Krishna, Sagar & Wiita 1995; Goyal et al. 2013). Online Table S2 (Column 5) compares the computed values of F_η for the two blazar DLCs of each session, with the critical value of $F (= F_c^\alpha)$ estimated for that session. The values of α are set at 0.05 and 0.01, corresponding to 95 per cent and 99 per cent confidence levels for INOV detection. If the computed F_η for a DLC of the target blazar exceeds F_c^α, the null hypothesis (i.e. no variability) is discarded at the corresponding confidence level. Thus, a DLC is classified as variable ('V') if the computed $F_\eta \geq F_c$ (0.99); probably variable ('PV') if the F_η falls between $F_c(0.95)$ and $F_c(0.99)$; and non-variable ('NV') if $F_\eta \leq F_c(0.95)$. Note that the target blazar in a session is designated as variable (V) only if both its DLCs (relative to the two comparison stars) belong to the 'V' category, and 'NV' if any of the two DLCs is of 'NV' type. The remaining sessions are designated 'PV'. The last column of the online Table S2 lists the session's averaged photometric accuracy, the 'photometric noise parameter' (PNP) $= \sqrt{\eta^2 \langle \sigma_{i,\text{err}}^2 \rangle}$, where $\eta = 1.54$.

5 RESULTS AND DISCUSSION

The present observations were mostly made under good sky conditions, using a 1.3-metre telescope located at a good site. With a typical threshold of $\psi \sim 2$ per cent for INOV detection, these observations compare well, both in sensitivity and cadence, with practically all other INOV observations reported in the literature. Yet, strikingly, INOV was not detected in any of the 24 monitoring sessions targeting our sample of six TeV-HBLs (online Figs S1–S6; Table S2). One possible exception is the session on 2021 Oct 10, during which a hint of gradual fading by ~ 2.5 per cent over 3 h was noticed for the $z = 0.314$ blazar J0507+6737. The fading was observed relative to both comparison stars which themselves remained steady throughout that session, as did the PSF (Fig. 1). Interestingly, this is the only blazar in our sample for which Piner & Edwards (2018) have reported a (mildly) superluminal motion at a high confidence level ($\beta_{app} = 2.23 \pm 0.44c$, i.e. 5.1σ, see Table 1). Even taking,

Table 1. The sample of six TeV-HBLs selected from Piner & Edwards (2018).

Blazar Name	RA (J2000) hh:mm:ss	Dec. (J2000) °: ′: ″	Redshift[a] z	m_r[b]	Apparent[c] jet speed β_{app}	Minimum polarization (per cent) (JD of observation)[d]	Maximum polarization (per cent) (JD of observation)[d]	Mean polarization[d] (per cent)	Median polarization[d] (per cent)	Number of polarization measurements[d]
J0136+3905 (RGB J0136+391)	01:36:32.60	+39:05:59.2	0.750[1]	15.83	$0.98 \pm 1.13^1 (< 1\sigma)$ $1.82 \pm 3.05^1 (< 1\sigma)$	1.4 ± 0.2 (2457336.4624)	4.1 ± 0.5 (2456853.5927)	2.37 ± 0.14	1.9	7
J0416+0105 (1ES 0414+009)	04:16:52.49	+01:05:23.9	0.287[2]	16.56	$0.03 \pm 0.58^1 (< 1\sigma)$	4.8 ± 0.9 (2456941.5946)	8.5 ± 0.4 (2457264.6115)	6.28 ± 0.28	5.9	4
J0507+6737 (1ES 050+675)	05:07:56.15	+67:37:24.3	0.314[3]	17.01	$2.23 \pm 0.44^1 (5.1\sigma)$ $7.92 \pm 3.51^1 (2.3\sigma)$	2.5 ± 0.6 (2456592.5206)	6.5 ± 0.4 (2456937.6025)	4.15 ± 0.14	4.0	15
J0650+2502 (1ES 0647 + 250)	06:50:46.49	+25:02:59.6	0.410[4]	14.61	$-3.13 \pm 1.67^1 (1.9\sigma)$	6.3 ± 0.4 (2456980.4321)	9.4 ± 0.4 (2457337.5394)	8.70 ± 0.20	9.3	5
J1427+2348 (PKS 1424+240)	14:27:00.39	+23:48:00.0	0.604[5]	14.11	$2.83 \pm 0.89^2 (3.2\sigma)$	0.3 ± 0.3 (2456780.4278)	10.6 ± 0.3 (2457228.2769)	5.76 ± 0.09	5.9	12
J1555+1111 (PG 1553+113)	15:55:43.04	+11:11:24.4	0.360[6]	14.28	$0.95 \pm 1.09^3 (< 1\sigma)$	0.2 ± 0.3 (2456519.2927)	9.6 ± 0.3 (2456914.227)	3.29 ± 0.02	2.9	284

[a]References for the redshift: 1. Neronov et al. (2015); 2. Chang et al. (2019); 3. O'Meara et al. (2021); 4. Kotilainen et al. (2011); 5. Paiano et al. (2017); 6. Neeleman et al. (2016). The lower limits on redshifts for J0136+3905, J0650+2502, J1427+2348, and J1555+1111 are also available in the ZBLLAC data base based on high SNR optical spectra (Landoni et al. 2020), consistent with their aforementioned redshifts.

[b]m_r is taken from Pan-STARRS survey (Chambers et al. 2016).

[c]References for the jet speed: 1. Piner & Edwards (2018); 2. Lister et al. (2019); 3. Tiet, Piner & Edwards (2012). The speeds are given in units of c and have been derived from the observed proper motions of the dominant VLBI knots.

[d]The polarization data have been taken from Blinov et al. (2021). The 'mean' values are our estimates based on the RoboPol data (Blinov et al. 2021).
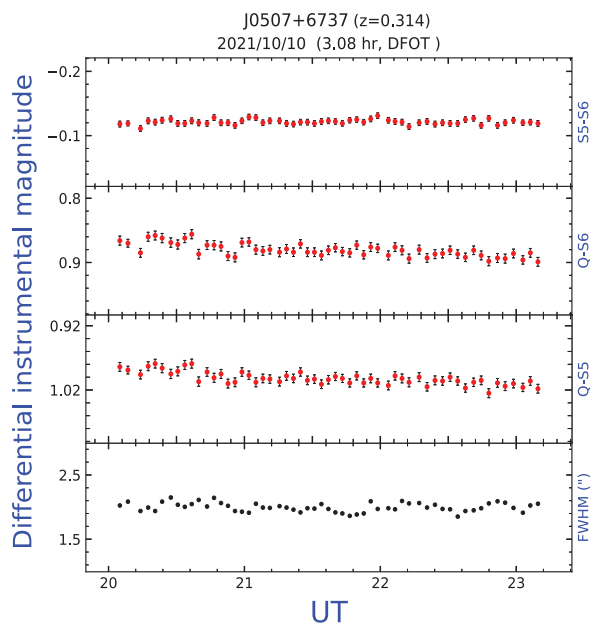
Figure 1. DLCs for the TeV-HBL J0507+6737 on 2021 Oct 10, on which the blazar showed a hint of fading by $\sim$2.5 per cent over 3 h, relative to both comparison stars. The upper plot gives the comparison star–star DLC and the middle two plots give the two blazar–star DLCs as defined in the labels on the right side. The lowest plot shows the seeing (PSF) variation during the session.

conservatively, this possible INOV detection as confirmed (despite its formal classification being 'non-variable', see online Table S2), the INOV duty cycle for our sample would still be only $\sim$4 per cent. This is miniscule in comparison to (i) the INOV DC of $\sim$60 per cent found for the sample of 13 TeV detected LBLs/FSRQs, which too mostly lie at $z > 0.3$ (Gopal-Krishna et al. 2011) and (ii) the INOV DC of $\sim$60–70 per cent generally found for LBLs (Heidt & Wagner 1998; Paliya et al. 2017). Thus, TeV-HBLs with parsec-scale jets dominated by subluminal (or mildly superluminal) radio knots, appears to be an extreme subclass of blazars with an INOV duty cycle bordering on zero. While such a possibility, i.e. INOV positively correlating with β_{app} has been hinted in some INOV studies (Stalin et al. 2005; Ojha et al. 2019), the present study demonstrates this link, for the first time with statistical robustness, based on an extensive INOV campaign focused on a blazar sample selected specifically for addressing this question (see Section 1). Here, it may be reiterated that our TeV-HBLs do exhibit the other common trait of blazars, namely a substantial fractional polarization ($p_{opt} > 3$ per cent, Table 1; Section 1). Not only is the maximum recorded p_{opt} consistent with this lower limit, but so is the mean value p_{opt} [except in the case of the blazar J0136+3905, but here too, p_{opt} was found to be above 3 per cent in two out of the total seven measurements available in the RoboPol survey (Blinov et al. 2021)[1]]. In this context, we further note that the high-polarization TeV-HBL J0416+0105 of our sample, having p_{opt} (mean) = 6.3 ± 0.3 per cent did not exhibit INOV (down to the 2

per cent detection limit), not only in the four sessions reported here, but also in the eight sessions (2016−2018) reported by Pandey et al. (2020).

It is also noteworthy that the non-detection of INOV even at $\sim$2 per cent level for essentially our entire sample of TeV-HBLs, also circumscribes the role of accretion disc flares (or instabilities) as a possible cause of INOV (e.g. Chakrabarti & Wiita 1993; Mangalam & Wiita 1993), at least in the case of geometrically thick radiatively inefficient discs that are supposed to fuel intrinsically low-power active galactic nuclei (AGN) like the TeV-HBLs being discussed here (Section 1).

As mentioned in Section 1, the two main factors perceived to be responsible for INOV of jet-dominated AGNs (blazars) are (i) injection/growth of turbulence within the jet plasma whose synchrotron emissivity and fractional polarization get enhanced while passing through one or more shocks (e.g. Marscher 2014 and references therein; Calafut & Wiita 2015; Pollack, Pauls & Wiita 2016; Webb et al. 2021; see also Laing 1980; Goyal et al. 2012); and (ii) the bulk Doppler factor δ_j of the post-shock turbulent plasma in the jet. While the former physical process is crucial for the origin of microvariability (INOV) of the jet's emission, the latter factor holds the key to the INOV detection (via a Doppler boost). Clearly, it is important to find observational basis for this scenario. A decade ago, Goyal et al. (2012) investigated the dependence of INOV on fractional optical polarization (p_{opt}), by carrying out sensitive, high-cadence optical monitoring of 21 radio-loud quasars, including 9 high- and 12 low-polarization quasars (HPQs and LPQs), taking the dividing line at the conventional $p_{opt} = 3$ per cent (e.g. Stockman, Moore & Angel 1984). Remarkably, the HPQ subset showed strong INOV (amplitude $\psi > 4$ per cent) on 11 out of 29 nights, in stark contrast to the LPQs for which strong INOV was observed on just 1 out of 44 nights. This clearly established a high p_{opt} as a key attribute of the radio quasars showing strong INOV. But, is this alone a sufficient marker for detection of strong INOV? What about the role of the aforementioned second factor, namely, δ_j? Indeed, an observational hint for such a correlation was noticed in a recent INOV study of three narrow-line Seyfert1 galaxies (Ojha et al. 2019). The results presented here place such a correlation on a statistically firm footing, for the first time, by focusing on an extreme subset of blazars, namely TeV-HBLs, whose nuclear radio jets exhibit only slow-moving (at most mildly superluminal) features, consistent with small Doppler boosting of their emission. For this subset, this work demonstrates an essentially total lack of INOV detection. This can be readily understood if the apparent kinematics of these dominant radio knots, which appear at most mildly superluminal, reflects the bulk motion of the underlying jet (at least the sheath layer), as argued by Lister et al. (2009a, b) and others (e.g. Kovalev et al. 2009; Lyutikov & Lister 2010). In this framework, compared to the highly superluminal radio knots typically observed in blazar jets, the dominant slow-moving radio knots observed in the VLBI jets of TeV-HBLs would have to be much more luminous intrinsically, in order to be detectable even without the benefit of a strong Doppler boosting. On the other hand, this would not be required in case the VLBI knots are mere 'patterns', kinematically decoupled from the underlying (much faster) jet, as suggested in several studies (e.g. Zensus 1997; Kellermann et al. 2004; Piner & Edwards 2018 and references therein). In that event, the observed brightness of the radio knots and the level of INOV originating in the jet's turbulent zone, would both be dictated by the beaming associated with the bulk velocity of the underlying jet (the, so-called, emission velocity of the jet, cf. Blandford & Königl 1979), despite little direct evidence for a relativistic flow coming from VLBI observations. The rather tight correlation of INOV with

---

[1]Note that, unless the number of measurements is very large, the maximum value of p_{opt} may be preferred over the mean value, as this would reduce the chance of missing out genuine blazars/HPQs since their polarization is known to vary and hence might average below the defining threshold of 3 per cent due to frequent dips (Impey, Lawrence & Tapia 1991; Chand & Gopal-Krishna 2022).

the apparent speed of the VLBI knots, as found here, suggests that at least the zone of turbulence within the (post-shock) jet-flow remains kinematically coupled to the (slow- moving) shock/knot, perhaps due to entanglement of the magnetic field lines, regardless of whether the observed kinematics of such shocks reflects the bulk speed of the underlying jet.

Finally, it should be emphasized that the very low INOV duty cycle inferred here for TeV-HBLs represents a 'population characteristics' and it is not meant to be a permanent metric for the INOV of any individual member of this class of blazars, e.g. by implying that no such blazar would ever exhibit a strong INOV. This important point has been underscored in Romero, Cellone & Combi (1999) by highlighting the case of the prominent TeV-HBL PKS 2155–304. This blazar, well-known for ultra-rapid variability of its TeV emission, is prone to slipping into prolonged spells of INOV quiescence, as noted by these authors. Another such example, the TeV-HBL PG1553+111, is a member of the present sample itself (Table 1). Its low INOV duty cycle implied by the non-detection of INOV on all four nights during 2022 (online Fig. S6) is statistically compatible with its recent study by Dhiman et al. (2023) in which INOV was detected on just 4 out of 27 nights of R-band monitoring during 2019. In contrast, during 2009–10, this blazar exhibited strong INOV ($\psi \gtrsim 5$ per cent) on all three nights it was monitored in R band (Gopal-Krishna et al. 2011). This indicates a transition to INOV quiescence, occurring somewhere between 2009–2010 and 2019–2022. Although a detailed comparison of this pattern with the jet's kinematic on parsec scale is currently lacking, it is interesting to note that the published MOJAVE images at 15 GHz do indicate a drop in the apparent speed of the dominant VLBI knots by a factor of ~ 3 over the period from 2008 to 2018 (see fig. 1 of Caproni et al. 2017), which is consistent with the above-inferred change in the INOV state (from high to low) of this TeV blazar. It would be desirable to garner further evidence on the question whether INOV state transitions are accompanied by a changing kinematics of the parsec-scale radio jets.

6 CONCLUSIONS

We have carried out an extensive, high-sensitivity intranight optical monitoring programme targeted on a well-defined sample of six TeV detected HBLs whose parsec-scale jets had been shown to be dominated by radio knots exhibiting either subluminal, or at most mildly superluminal motion. An essentially zero INOV duty cycle is estimated here from the 24 monitoring sessions devoted to these TeV-HBLs, despite their exhibiting fairly high degree of optical polarization. This INOV duty cycle is at least an order of magnitude lower than that typical of radio-selected blazars (LBLs, whose parsec-scale jets are usually dotted with highly superluminal knots, e.g. Britzen et al. 2007; Cohen et al. 2007; Lister et al. 2009a; Jorstad et al. 2017). Thus, TeV-HBLs with slow-moving VLBI knots are clearly identified for the first time as an extreme subpopulation of blazars, from the perspective of INOV. Their highly subdued INOV, as found here, demonstrates that the presence of dominant superluminal radio knot(s) in the parsec-scale jet constitutes a key diagnostic for INOV detection and while a high degree of optical polarization is also an important marker, as shown in Goyal et al. (2012), it alone is not a sufficient diagnostic for INOV detection.

DATA AVAILABILITY

The data used in this study will be shared on reasonable request to the corresponding author.

REFERENCES

Abdo A. A. et al., 2010, ApJ, 716, 30
Antonucci R., 1993, ARA&A, 31, 473
Barthel P. D., 1989, ApJ, 336, 606
Blandford R. D., Königl A., 1979, ApJ, 232, 34
Blandford R., Meier D., Readhead A., 2019, ARA&A, 57, 467
Blinov D. et al., 2021, MNRAS, 501, 3715
Britzen S. et al., 2007, A&A, 472, 763
Britzen S. et al., 2021, MNRAS, 503, 3145
Britzen S., Gopal-Krishna, Kun E., Hector O., Ilya N. P., Frederic J., González J. B., Paneque D., 2023, Universe, 9, 115
Browne I. W. A., 1989, in Maraschi L., Maccacaro T., Ulrich M.-H.eds., BL Lac Objects, Vol. 334. Springer-Verlag, Berlin, p. 401
Bruni G. et al., 2021, A&A, 654, A27
Calafut V., Wiita P. J., 2015, JA&A, 36, 255
Caproni A., Abraham Z., Motter J. C., Monteiro H., 2017, ApJ, 851, L39
Cellone S. A., Romero G. E., Combi J. A., 2000, AJ, 119, 1534
Chakrabarti S. K., Wiita P. J., 1993, ApJ, 411, 602
Chambers K. C., et al., 2016, preprint (arXiv:1612.05560)
Chand K., Gopal-Krishna, 2022, MNRAS, 516, L18
Chand K., Gopal-Krishna, Omar A., Chand H., Mishra S., Bisht P. S., Britzen S., 2022, MNRAS, 511, 13
Chang Y. L., Arsioli B., Giommi P., Padovani P., Brandt C. H., 2019, A&A, 632, A77
Chiaberge M., Capetti A., Celotti A., 1999, A&A, 349, 77
Chiaberge M., Celotti A., Capetti A., Ghisellini G., 2000, A&A, 358, 104
Cohen M. H., Lister M. L., Homan D. C., Kadler M., Kellermann K. I., Kovalev Y. Y., Vermeulen R. C., 2007, ApJ, 658, 232
de Diego J. A., 2010, AJ, 139, 1269
Dhiman V. et al., 2023, MNRAS, 519, 2796
Fanaroff B. L., Riley J. M., 1974, MNRAS, 167, 31P
Ghisellini G., Celotti A., 2001, MNRAS, 327, 739
Ghisellini G., Tavecchio F., Chiaberge M., 2005, A&A, 432, 401
Ghisellini G., Maraschi L., Tavecchio F., 2009, MNRAS, 396, L105
Giommi P., Padovani P., Polenta G., Turriziani S., D'Elia V., Piranomonte S., 2012, MNRAS, 420, 2899
Giroletti M. et al., 2004, ApJ, 600, 127
Giroletti M., Giovannini G., Taylor G. B., Falomo R., 2006, ApJ, 646, 801
Gopal-Krishna, Wiita P. J., 2018, Bull. Soc. R. Sci. Liege, 87, 281
Gopal-Krishna, Sagar R., Wiita P. J., 1995, MNRAS, 274, 701
Gopal-Krishna, Goyal A., Joshi S., Karthick C., Sagar R., Wiita P. J., Anupama G. C., Sahu D. K., 2011, MNRAS, 416, 101
Gopal-Krishna, Chand K., Chand H., Negi V., Mishra S., Britzen S., Bisht P. S., 2023, MNRAS, 518, L13
Goyal A., Gopal-Krishna, Wiita P. J., Anupama G. C., Sahu D. K., Sagar R., Joshi S., 2012, A&A, 544, A37
Goyal A., Mhaskey M., Gopal-Krishna, Wiita P. J., Stalin C. S., Sagar R., 2013, JA&A, 34, 273
Hardcastle M. J., Worrall D. M., Birkinshaw M., Canosa C. M., 2003, MNRAS, 338, 176
Heidt J., Wagner S. J., 1998, A&A, 329, 853
Impey C. D., Lawrence C. R., Tapia S., 1991, ApJ, 375, 46
Janssen M. et al., 2021, Nat. Astron., 5, 1017
Jorstad S. G. et al., 2017, ApJ, 846, 98
Kellermann K. I. et al., 2004, ApJ, 609, 539
Kotilainen J. K., Hyvönen T., Falomo R., Treves A., Uslenghi M., 2011, A&A, 534, L2

Kovalev Y. Y. et al., 2009, ApJ, 696, L17

Laing R. A., 1980, MNRAS, 193, 439

Laing R. A., Parma P., de Ruiter H. R., Fanti R., 1999, MNRAS, 306, 513

Laing R. A., Guidetti D., Bridle A. H., Parma P., Bondi M., 2011, MNRAS, 417, 2789

Landoni M., Falomo R., Paiano S., Treves A., 2020, ApJS, 250, 37

Lister M. L. et al., 2009a, AJ, 138, 1874

Lister M. L., Homan D. C., Kadler M., Kellermann K. I., Kovalev Y. Y., Ros E., Savolainen T., Zensus J. A., 2009b, ApJ, 696, L22

Lister M. L. et al., 2019, ApJ, 874, 43

Lyutikov M., Lister M., 2010, ApJ, 722, 197

Mangalam A. V., Wiita P. J., 1993, ApJ, 406, 420

Marscher A. P., 2014, ApJ, 780, 87

Marscher A., 2016, Galaxies, 4, 37

Meyer E. T., Fossati G., Georganopoulos M., Lister M. L., 2011, ApJ, 740, 98

Mishra S., Gopal-Krishna, Chand H., Chand K., Ojha V., 2019, MNRAS, 489, L42

Mishra S., Gopal-Krishna, Chand H., Chand K., Kumar A., Negi V., 2021, MNRAS, 507, L46

Neeleman M., Prochaska J. X., Ribaudo J., Lehner N., Howk J. C., Rafelski M., Kanekar N., 2016, ApJ, 818, 113

Neronov A., Semikoz D., Taylor A. M., Vovk I., 2015, A&A, 575, A21

O'Meara J. M., Lehner N., Howk J. C., Prochaska J. X., 2021, AJ, 161, 45

Ojha V., Gopal-Krishna, Chand H., 2019, MNRAS, 483, 3036

Owen F. N., Hardee P. E., Cornwell T. J., 1989, ApJ, 340, 698

Padovani P., Giommi P., 1995, MNRAS, 277, 1477

Paiano S., Landoni M., Falomo R., Treves A., Scarpa R., Righi C., 2017, ApJ, 837, 144

Paliya V. S., Stalin C. S., Ajello M., Kaur A., 2017, ApJ, 844, 32

Pandey A., Gupta A. C., Damljanovic G., Wiita P. J., Vince O., Jovanovic M. D., 2020, MNRAS, 496, 1430

Piner B. G., Edwards P. G., 2018, ApJ, 853, 68

Piner B. G., Pant N., Edwards P. G., Wiik K., 2009, ApJ, 690, L31

Piner B. G., Pant N., Edwards P. G., 2010, ApJ, 723, 1150

Pollack M., Pauls D., Wiita P. J., 2016, ApJ, 820, 12

Romero G. E., Cellone S. A., Combi J. A., 1999, A&AS, 135, 477

Sagar R. et al., 2011, Curr. Sci., 101, 1020

Sbarrato T., Padovani P., Ghisellini G., 2014, MNRAS, 445, 81

Stalin C. S., Gupta A. C., Gopal-Krishna, Wiita P. J., Sagar R., 2005, MNRAS, 356, 607

Stetson P. B., 1987, PASP, 99, 191

Stetson P. B., 1992, in Worrall D. M., Biemesderfer C., Barnes J., eds, ASP Conf. Ser. Vol. 25, Astronomical Data Analysis Software and Systems I. Astron. Soc. Pac., San Francisco, p. 297

Stickel M., Padovani P., Urry C. M., Fried J. W., Kuehr H., 1991, ApJ, 374, 431

Stockman H. S., Moore R. L., Angel J. R. P., 1984, ApJ, 279, 485

Swain M. R., Bridle A. H., Baum S. A., 1998, ApJ, 507, L29

Tadhunter C., 2016, A&AR, 24, 10

Tiet V. C., Piner B. G., Edwards P. G., 2012, preprint (arXiv:1205.2399)

Trussoni E., Capetti A., Celotti A., Chiaberge M., Feretti L., 2003, A&A, 403, 889

Ulrich M.-H., Maraschi L., Urry C. M., 1997, ARA&A, 35, 445

Urry C. M., Padovani P., 1991, ApJ, 371, 60

Urry C. M., Padovani P., 1995, PASP, 107, 803

Wagner S. J., Witzel A., 1995, ARA&A, 33, 163

, in Wakely S. P., Horan D., Caballero R., D'Olivo J. C., 2008, eds., International Cosmic Ray Conference. p. 1341

Wardle J. F. C., Moore R. L., Angel J. R. P., 1984, ApJ, 279, 93

Webb J. R. et al., 2021, Galaxies, 9, 114

Zensus J. A., 1997, ARA&A, 35, 607

SUPPORTING INFORMATION

Supplementary data are available at *MNRASL* online.

Figure S1. DLCs for the six TeV-HBLs in our sample.
Figure S2. Same as in Fig. S1.
Figure S3. Same as in Fig. S1.
Figure S4. Same as in Fig. S1.
Figure S5. Same as in Fig. S1.
Figure S6. Same as in Fig. S1.
Table S1. Basic parameters of selected comparison stars for six TeV-HBLs in our sample.
Table S2. Result of variability analysis of six TeV-HBLs in our sample (taking $\eta = 1.54$).

Please note: Oxford University Press is not responsible for the content or functionality of any supporting materials supplied by the authors. Any queries (other than missing material) should be directed to the corresponding author for the article.

This paper has been typeset from a TeX/LaTeX file prepared by the author.